

## Femtosecond four-wave-mixing studies of nearly homogeneously broadened excitons in GaN

A. J. Fischer, W. Shan, G. H. Park, and J. J. Song

*Department of Physics and Center for Laser Research, Oklahoma State University, Stillwater, Oklahoma 74078*

D. S. Kim and D. S. Yee

*Department of Physics, Seoul National University, Seoul 151-742, Korea*

R. Horning and B. Goldenberg

*Honeywell Technology Center, Plymouth, Minnesota 55441*

(Received 10 December 1996)

Femtosecond degenerate four-wave-mixing (FWM) is used to study coherent dynamics of excitons in GaN epilayers. Spectrally resolved (SR) FWM data are dominated by the *A* and *B* intrinsic excitonic resonances. SR FWM combined with time-integrated (TI) FWM demonstrates that the excitonic resonances are nearly homogeneously broadened even at low temperature. The temperature-dependent dephasing rate is used to deduce exciton-phonon interaction rates. TI FWM shows a strong beating between the *A* and *B* excitons and the beats are shown to be true quantum beats. In addition, a  $180^\circ$  phase shift in the quantum beating was observed when the polarization geometry was changed from collinear to cross linear. [S0163-1829(97)06627-7]

Recently, there has been tremendous interest in GaN and related materials, due to its ability to emit light in the blue/UV region.<sup>1</sup> Many types of linear optical spectroscopy have been used to study these wide-band-gap semiconductors.<sup>2</sup> Nevertheless, significant uncertainties still remain regarding the fundamental band edge transitions in GaN. For instance, due to strong absorption in GaN and poor sample quality for thin layers ( $< 1 \mu\text{m}$ ), unambiguous determination of the exciton linewidth as a function of temperature by absorption is difficult, and as a result, exciton-phonon interaction rates are not well known. In addition, clear evidence of free excitons in the absorption spectra is still lacking.

Another area of intense research activity has been the coherent spectroscopy of semiconductors and their quantum wells, stimulated in part by the ready availability of tunable femtosecond laser sources. Extensive studies have been performed on GaAs, ZnSe, and related materials and their quantum wells in the coherent regime.<sup>3,4</sup> However, up to now, no studies have been performed on GaN in the femtosecond coherent regime.

In this paper, we present the results of femtosecond four-wave-mixing (FWM) studies on nearly homogeneously broadened excitons in a high-quality GaN epilayer sample. We have performed time-integrated (TI) FWM and spectrally resolved (SR) FWM as a function of temperature and polarization. From these studies, we have determined exciton-acoustic-phonon and exciton-optical-phonon coupling constants. TI FWM displays well-defined beating between the *A* and the *B* excitons, and SR FWM demonstrates that the beating is due to true quantum beats between these two modes, and not due to the so-called polarization beat.<sup>5</sup> In addition, the quantum beat between the *A* and the *B* excitons shows a  $180^\circ$  phase shift between the collinear and the cross-linear polarization geometries. This is analogous to the heavy-hole (HH) and light-hole (LH) exciton quantum beat

in GaAs quantum wells, which also shows a  $180^\circ$  phase shift between the two polarization geometries.<sup>6</sup>

We used the second harmonic of a self-mode-locked Ti:sapphire laser in the high-energy region of the tuning curve (700 nm). The second harmonic of the 100-fs pulses resonantly excites intrinsic excitons in the GaN epilayer. The  $7.2\text{-}\mu\text{m}$ -thick epilayer was grown with the wurtzite structure on a *c*-phase sapphire substrate using metalorganic chemical vapor deposition (MOCVD). The valence-band degeneracy for wurtzite crystals is removed by crystal field splitting and spin-orbit interaction. As shown in the inset of Fig. 2(a), the two lowest-energy transitions at the  $\Gamma$  point are the  $\Gamma_9^V - \Gamma_7^C$  exciton (*A* exciton transition) and the  $\Gamma_7^V$  (upper band)- $\Gamma_9^C$  exciton (*B* exciton transition). FWM was performed on the *A* and *B* exciton transitions in the reflection geometry with an average power per beam of about 1 mW focused onto a  $100\text{-}\mu\text{m}$  spot.

In Fig. 1(a), TI FWM data are shown at three different temperatures ( $T = 10, 70,$  and  $190$  K). The laser was tuned near resonance with the *B* exciton, and the weak beating at 10 K is a result of the excitation of a small *A* exciton component. At 190 K, the FWM signal is nearly time-resolution limited. The decay time at each temperature was fit to a single exponential decay to determine the decay rate as a function of temperature. The homogeneous linewidth can be determined from the relation  $\Gamma_{\text{hom}} = 2\hbar/T_2$ , where  $T_2$  is the pure dephasing time. In order to determine  $T_2$ , we need to know if the resonances are predominantly homogeneously or inhomogeneously broadened. This is because the FWM decay time  $\tau_{\text{FWM}}$  is equal to  $T_2/2$  in the homogeneously broadened limit and  $T_2/4$  in the inhomogeneously broadened limit.<sup>7</sup> As discussed below, SR FWM is used to show that the excitonic resonances studied here are nearly homogeneously broadened. Figure 1(b) shows the homogeneous linewidth plotted as a function of temperature assuming homogeneous

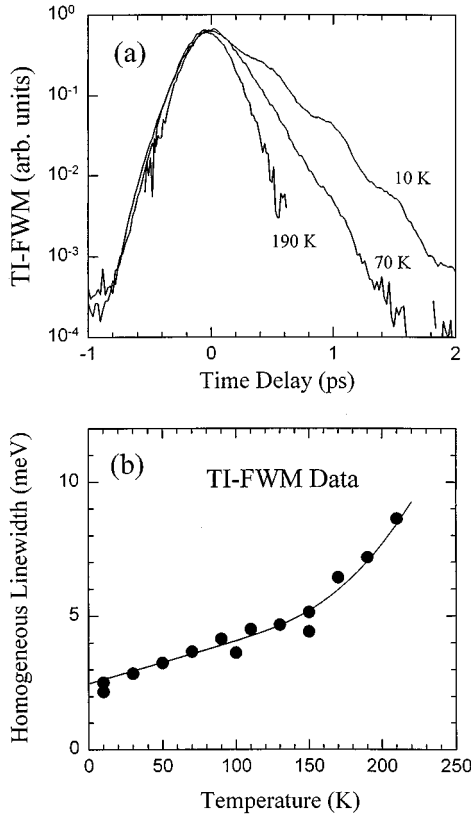


FIG. 1. (a) Time-integrated four-wave-mixing (TI FWM) signal in the reflection geometry near the  $B$ -exciton resonance at 10, 70, and 190 K for a  $7.2\text{-}\mu\text{m}$  epilayer of GaN grown on sapphire. (b) Homogeneous linewidth plotted as a function of temperature. The solid line is a least-squares fit to Eq. (1) with parameters  $\gamma=16\text{ }\mu\text{eV/K}$  and  $\Gamma_{\text{LO}}=390\text{ meV}$ .

broadening. Initially, the rate is linear with  $T$ , but begins to be superlinear starting from about 150 K. This indicates the dominance of the acoustic phonons as the scattering mechanisms for the dephasing of excitons at low temperature. At higher temperature, it is expected that optical phonons begin to contribute. We fit the homogeneous linewidth data in Fig. 2(b) to the following standard formula:<sup>8,9</sup>

$$\Gamma = \Gamma_0 + \gamma T + \frac{\Gamma_{\text{LO}}}{\exp(E_{\text{LO}}/k_B T) - 1}, \quad (1)$$

where  $\Gamma_0$ ,  $\gamma$ , and  $\Gamma_{\text{LO}}$  are constants to be determined from the fit, and  $E_{\text{LO}}$  and  $k_B$  are, respectively, the optical phonon energy of GaN (91.7 meV) and Boltzmann's constant. The best fit is the solid line in Fig. 1(b), achieved with the fitting parameters:  $\Gamma_0=2.4\text{ meV}$ ,  $\gamma=16\text{ }\mu\text{eV/K}$ , and  $\Gamma_{\text{LO}}=390\text{ meV}$ . These values are much larger than those for GaAs and GaAs quantum wells.<sup>9</sup> This is not so surprising, for GaN has larger effective masses for both electrons and holes in comparison with GaAs, and thus a much larger density of states. On the other hand,  $\gamma$  is comparable to that of ZnSe and  $\text{Zn}_x\text{Cd}_{1-x}\text{Se}$  quantum wells, whereas  $\Gamma_{\text{LO}}$  is still much larger than that of ZnSe and related materials.<sup>4</sup> This is an interesting point, for the density of states of ZnSe as well as its polarity are comparable to those of GaN. The much larger  $\Gamma_{\text{LO}}$  for GaN should in part be due to the much larger  $E_{\text{LO}}$  of GaN in comparison to ZnSe (91 versus 30 meV). In addition,

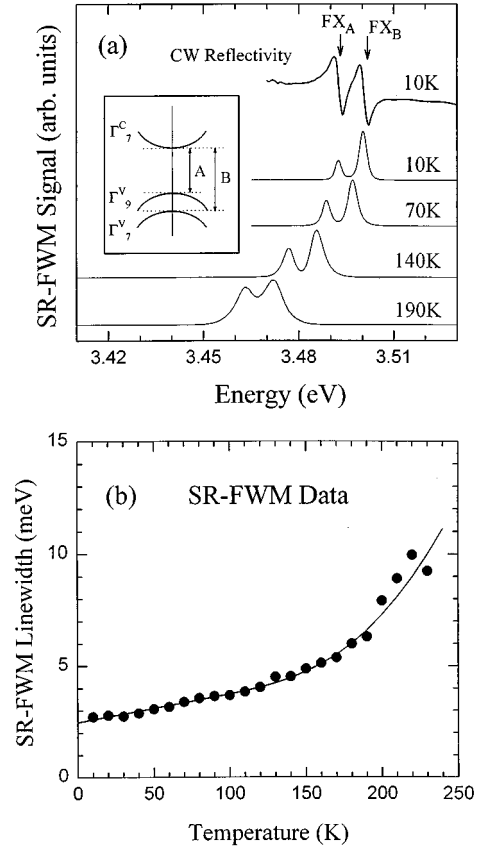


FIG. 2. (a) Spectrally resolved (SR) FWM signals from the  $A$  and  $B$  exciton resonances near zero delay at 10, 50, 100, 150, and 190 K plotted together with continuous-wave reflectivity data from the same sample. The  $A$  ( $\text{FX}_A$ ) and  $B$  ( $\text{FX}_B$ ) intrinsic free excitons are labeled and the inset shows the excitonic band structure. The  $B$ -exciton linewidth of 2.5 meV (full width at half maximum) at 10 K together with the FWM decay time of 300 fs ( $T_s = 2\tau_{\text{FWM}} \Rightarrow \Gamma_{\text{hom}} = 2.2\text{ meV}$ ) indicate that the excitons in our samples are mostly homogeneously broadened even at low temperature. (b) SR FWM linewidth of the  $B$  exciton plotted as a function of temperature. The solid line is a least-squares fit to Eq. (1) with parameters  $\gamma=13\text{ }\mu\text{eV/K}$  and  $\Gamma_{\text{LO}}=470\text{ meV}$ .

it is possible that a larger deformation potential interaction, which may account for a significant fraction of  $\Gamma_{\text{LO}}$  in addition to the Fröhlich interaction, is responsible for the larger  $\Gamma_{\text{LO}}$ .

To determine whether the excitons are homogeneously or inhomogeneously broadened, we performed SR FWM. The advantage of SR FWM is that it can give the exciton linewidths without any background, which plagues the analysis of absorption experiments. In addition, for high-quality, relatively thick epilayer samples, it is virtually impossible to perform absorption. In Fig. 2(a), SR FWM data at zero delay are plotted at several temperatures. Both the  $A$  and  $B$  excitons are clearly present, and the SR FWM data shown in Fig. 2(a) represent a very clear demonstration of the  $A$  and the  $B$  excitons without the interference of bound excitons that make the interpretation of photoluminescence spectra difficult. The SR FWM linewidth at 10 K, the lowest temperature of our experiments, is about 2.5 meV for the  $B$  exciton, and about 2.1 meV for the  $A$  exciton. From TI FWM and the fit

shown in Fig. 1(a), the homogeneous linewidth in the low-temperature limit is about 2.4 meV assuming homogeneous broadening, and 1.2 meV assuming inhomogeneous broadening. Therefore, even in the low-temperature limit, the *minimum* homogeneous linewidth of our excitons is about half the total linewidth observed in SR FWM. On the other hand, the observed linewidth is nearly equal to what is expected in the homogeneously broadened limit. At higher temperature, there is no doubt that the excitons we probe by FWM are predominantly homogeneously broadened. From these observations, we conclude that our excitons can be considered mostly homogeneously broadened even at low temperature.

Figure 2(b) shows the SR FWM linewidth of the *B* exciton obtained from a fit to the temperature-dependent data presented in Fig. 2(a). The solid curve is a fit to the phonon broadening equation [Eq. (1)] where the fit parameters are given by  $\Gamma_0 = 2.5$  meV,  $\gamma = 13$   $\mu\text{eV/K}$ , and  $\Gamma_{\text{LO}} = 470$  meV. Since the time-resolved data of Fig. 1 become time-resolution limited above 210 K, the SR FWM data give more reliable values of the exciton-phonon coupling constants, especially  $\Gamma_{\text{LO}}$ . Note, however, that the values from both SR FWM and TI FWM are quite close. Recent linear absorption measurements also give values of  $\Gamma_0 = 10$  meV,  $\gamma = 15$   $\mu\text{eV/K}$ , and  $\Gamma_{\text{LO}} = 375$  meV.<sup>10</sup> The values obtained from a fit to absorption data contain the most error since a large background of free carrier absorption must be subtracted. For SR FWM measurements, on the other hand, it is known that the excitonic contribution is several orders of magnitude larger than the free carrier contribution. Therefore, the values obtained from SR FWM measurements are the most reliable and indicate that the exciton-phonon coupling constants in GaN are quite large.

The relatively fast scattering at low temperature is most likely due to scatterings with macroscopic variations in sample quality or impurity scattering. On the other hand, since the total linewidth is roughly the sum of the homogeneous and the inhomogeneous broadenings,<sup>11</sup> we can put the upper limit to the inhomogeneous broadening in our sample caused by variations in sample quality. For both the *A* and the *B* excitons, it is less than 1.5 meV, and most likely in the range of a few tenths of a meV. Therefore, with further reduction of the defect density, achieving GaN exciton linewidths of less than 1 meV should be possible.

We now discuss the quantum beat between the *A* and the *B* excitons observed by TI and SR FWM. As shown in Fig. 3, when we tune the laser roughly in the middle of the *A* and *B* exciton, well-defined beating, whose period coincides with  $(E_B - E_A)/h$ , is observed ( $E_A, E_B$  is the energy of the *A* and the *B* excitons observed in SR FWM, respectively). However, the beating observed in TI FWM in itself does not imply the existence of charge oscillation in the coherent superposition of *A* and *B* excitons. To prove that it is really a quantum beat, we probe the relative phase of the beating at different energies.<sup>5</sup> In Fig. 3, TI FWM is plotted as a function of delay for several different energy positions across the *B* exciton resonance. The phases are completely in synch at all the energies, which indicates that the beating we observe in TI FWM is indeed due to the coherent superposition of the *A* and the *B* excitons.

Having established the quantum nature of the beating observed in TI FWM, we now turn our attention to the polar-

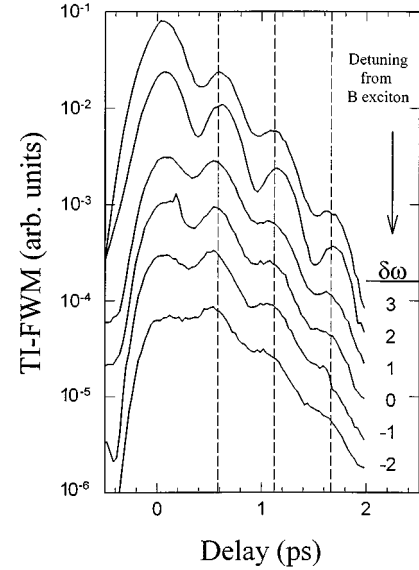


FIG. 3. TI FWM data at 10 K at different detunings  $\delta\omega = \hbar(\omega_d - \omega_2)$  meV around the *B* exciton. ( $\omega_d$  is the detection frequency). The laser is set to excite both the *A* and *B* resonances. The fact that we see no phase shift as a function of energy position across the *B* exciton resonance indicates that the observed beats are true quantum beats. Different temperatures are offset for clarity.

ization dependence of the quantum beat. In Fig. 4, TI FWM in both the collinear (solid lines) and the cross-linear (dotted lines) polarization geometries are shown. The maxima at one geometry correspond to the minima at the other, which indicates the existence of a  $180^\circ$  phase shift between the quantum beats. Similar observations have been made in the case of the HH-LH quantum beat in GaAs quantum wells, and was theoretically described by including the total angular momentum for the conduction band ( $J = \frac{1}{2}$ ) and valence band ( $J = \frac{3}{2}$ ) in the optical Bloch equations.<sup>6</sup> In our case, the phase shift is likely to be caused by the different spin states of holes in the  $\Gamma_7$  and the  $\Gamma_9$  valence bands.

In conclusion, we have performed femtosecond coherent spectroscopy on excitons in a high-quality GaN epilayer

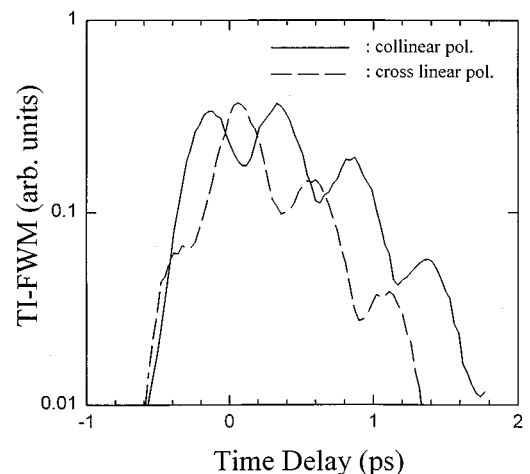


FIG. 4. TI FWM signal at 10 K for collinear (solid) and cross-linear (dashed) polarization geometries.

grown on a sapphire substrate. By the combined analysis of the TI FWM and SR FWM, we found that our excitons are nearly homogeneously broadened. We have deduced the exciton-phonon interaction rates, and observed a beating in TI FWM that we identified as a quantum beat between the *A* and the *B* excitons. Finally, we observed a clear 180° phase shift between the quantum beats in the collinear and the cross-linear polarization geometries, which we explain

by differences between total angular momentum of the conduction band and the *A* and *B* valence bands.

We would like to thank Dr. L. J. Sham for helpful discussions. This work was supported by a joint grant of NSF and KOSEF (965-0200-003-2). The work at OSU was also supported by DARPA and ARO and the work at SNU was supported by the Ministry of Education (BSRI96-7401).

- 
- <sup>1</sup>S. Nakamura, M. Senoh, S. Nagahama, N. Iwasa, T. Yamada, T. Matsushita, H. Kiyoku, and Y. Sugimoto, *Jpn. J. Appl. Phys.* **2**, Lett. **235**, L74 (1996).
- <sup>2</sup>W. Shan, T. Schmidt, X. H. Yang, J. J. Song, and B. Goldenberg, *J. Appl. Phys.* **79**, 3691 (1996); G. D. Chen, M. Smith, J. Y. Lin, H. X. Jiang, A. Salvador, B. N. Sverdlov, A. Botchkarev, and H. Morkoç, *ibid.* **79**, 2675 (1996).
- <sup>3</sup>K. Leo, E. O. Göbel, T. C. Damen, J. Shah, S. Schmitt-Rink, W. Schäfer, J. F. Müller, K. Köhler, and P. Ganser, *Phys. Rev. B* **44**, 5726 (1991); Th. Östreich, K. Schönhammer, and L. J. Sham, *Phys. Rev. Lett.* **74**, 4698 (1995); E. J. Mayer, G. O. Smith, V. Heuckeroth, J. Kuhl, K. Bott, A. Schulze, T. Meier, D. Benndardt, S. W. Koch, P. Thomas, R. Hey, and K. Ploog, *Phys. Rev. B* **50**, 14 730 (1994); Y. Z. Hu, R. Binder, S. W. Koch, S. T. Cundiff, H. Wang, and D. G. Steel, *ibid.* **49**, 14 382 (1994).
- <sup>4</sup>A. J. Fischer, D. S. Kim, J. Hays, W. Shan, J. J. Song, D. B. Eason, J. Ren, J. F. Schetzina, H. Luo, J. K. Furdyna, Z. Q. Zhu, T. Yao, and W. Schäfer, *Phys. Rev. Lett.* **73**, 2368 (1994).
- <sup>5</sup>V. G. Lyssenko, J. Erland, I. Balslev, K.-H. Pantke, B. S. Razbirin, and J. M. Hvam, *Phys. Rev. B* **48**, 5720 (1993).
- <sup>6</sup>S. Schmitt-Rink, D. Bennhardt, V. Heuckeroth, P. Thomas, P. Haring, G. Maidorn, H. Bakker, K. Leo, D. S. Kim, J. Shah, and K. Köhler, *Phys. Rev. B* **46**, 10 460 (1992).
- <sup>7</sup>T. Yajima and Y. Taira, *J. Phys. Soc. Jpn.* **47**, 160 (1980).
- <sup>8</sup>J. Lee, E. Koteles, and M. O. Vassell, *Phys. Rev. B* **33**, 5512 (1986).
- <sup>9</sup>D. S. Kim, J. Shah, J. E. Cunningham, T. C. Damen, W. Schäfer, M. Hartmann, and S. Schmitt-Rink, *Phys. Rev. Lett.* **68**, 1006 (1992).
- <sup>10</sup>A. J. Fischer, W. Shan, J. J. Song, Y. C. Chang, R. Horning, and B. Goldenberg (unpublished).
- <sup>11</sup>S. Rudin, T. L. Reinecke, and B. Segall, *Phys. Rev. B* **42**, 11 218 (1992).